Investigating The Thermal Performance and Magneto Nanofluid Flow Behaviour for Engineering Application

Mukesh Kumar Sharma[1], Susheela Chaudhary[2]
[1]*Ph.D Scholar, Affiliation Address: Pandit Deendayal Upadhyay Shekhawati University, Sikar, Rajasthan, India*
[2]*Professor, Shri Kalyan Rajkiya Kanya Mahavidyalaya, Sikar, Rajasthan, India*

***Abstract*—This present study is a work on the thermal performance and flow characteristics of magneto-nanofluids to be used in advanced engineering. Nanofluids that are made through the suspension of nanoparticles in normal base fluids have a higher thermal conductivity and heat transfer efficiency than the normal fluids. The study incorporates the concepts of magnetohydrodynamic (MHD) in order to understand the impact of an external magnetic field on fluid dynamics and thermal properties. A simple two-dimensional laminar model of boundary layer is formulated which includes mass, momentum, and energy equations, and effective thermophysical variables. Velocity and temperature profiles are obtained using similarity transformations and numerical methods (RKF-45 using shooting method). The parametric analysis helps to reveal the impact of magnetic parameter, concentration of nanoparticle, and Prandtl number on the heat transfer and flow dynamics. It has been found that magnetic fields could be successfully used in the treatment of flow behaviour and to produce better thermal performance.**

***Index Terms*—Magneto-nanofluid, Heat transfer enhancement, Magnetohydrodynamics (MHD), Thermal performance, Boundary layer flow, Nanoparticle concentration**

I. INTRODUCTION

The researchers are coming up with next generation heat transfer fluids since in the current engineering, high efficiency thermal systems are required in the current engineering projects. The thermal performance of traditional fluids, which include water and ethylene glycol and oils, becomes limited in high-heat-flux situations that arise in energy systems and aerospace components and microelectronics cooling and nuclear reactors and chemical processing equipment [1]. The development of nanofluids, which are created by mixing nano-scale particles with base fluids, provides an effective method to enhance thermal transport properties and boost overall system performance [2]. The image in Figure1 demonstrates how researchers create nanofluids through the process of mechanical stirring, which enables nanoparticles to disperse evenly into a base fluid, followed by ultrasonication for achieving stable particle suspension. The two-step process establishes equal particle distribution while it also decreases particle clumping and improves thermo physical characteristics, which result in better heat transfer capability. Figure 1 represents the Conventional fluid vs. nanofluid thermal conductivity enhancement.

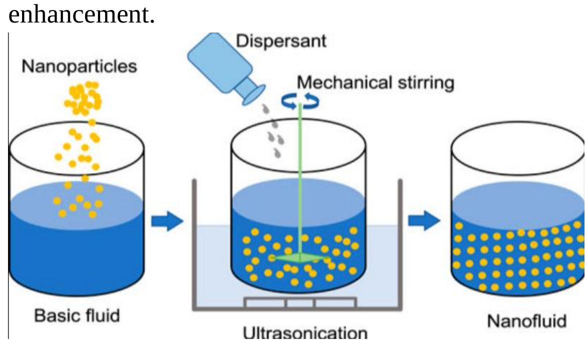

Figure 1. Conventional fluid vs. nanofluid thermal conductivity enhancement [3]

Copper (Cu), aluminum oxide (Al_2O_3), titanium dioxide (TiO_2), graphene and carbon nanotubes (NPTs) are of high importance in the sense that they are nanoparticles that increase the effective thermal conductivity, convective heat transfer coefficient and the energy transport capacity of the host fluid [4]. Nanoparticles have an exceptionally high surface-to-volume ratio that enables the solid particles to interact better with the liquid that surrounds them, which leads to quicker heat diffusion and reduced thermal resistance [5]. Consequently, nanofluids have higher thermal performance than classical fluids, and are therefore suitable in compact heat exchangers, solar collectors, medical devices, and electronic cooling applications where space and efficiency are very important in design [6].

Simultaneously with the studies done on nanofluids, "magnetohydrodynamics (MHD)" the science of electrically conductive fluid flow under magnetic field influences has become a significant point of interest in regulating the behavior of fluid motion as well as heat transfer [7]. Lorentz forces are produced when a magnetic field is applied on a conducting nanofluid; this interacts with the flow field and changes the distribution of velocity, the thickness of the boundary layers, and thermal gradient [8]. It is a magnetic control that allows the fine control of fluid flow without any mechanical contact, and it is useful in the system, where contamination, wear, or mechanical complexity needs to be reduced. Combination of magnetic effects and nanofluid technology has therefore led to the introduction of the term magneto-nanofluids, which entails the improved thermal behavior coupled with the manipulation of flow behaviour [9].

The analysis of the magneto nanofluids flow behaviour is specifically associated with the engineering practice in terms of electromagnetic pumps, nuclear reactor cooling, metallurgy, microfluidic, magnetic drug targeting and the use of renewable energy sources such as solar thermal collector [10]. In these systems the magnetic forces, viscous effects, diffusion of nanoparticles and thermal transport are coupled causing interactions which are multi-physical and complex [11]. The strength of the magnetic field, nanoparticle volume fraction, Brownian motion, thermo phoresis and fluid viscosity are some of the parameters that contribute greatly in the determination of the heat transfer enhancement and flow stability. These interactions are crucial to designing systems that are highly thermal efficient and are sufficiently controllable, and have minimal energy losses [12].

The recent trends in computational techniques and experimental schemes have enabled to investigate the magneto nanofluid dynamics in more details with various boundary conditions like stretching surfaces, porous materials, rotating system and convective heating situations [13]. Mathematical modeling of conservation laws of mass, momentum and energy and Maxwell electromagnetic equations provide information on the velocity profiles, temperature distributions, entropy generation and thermal performance indices. Such analyses are crucial in the prediction of system behavior prior to the actual implementation on the real-life setting and also by the optimization of the engineering designs [14].

Though this has been done to an excellent level, still there are certain problems that can be faced in the real-life use of magneto nanofluids. Nanoparticle agglomeration, stability, pressure drop, trade-off with thermal enhancement and pumping power issues must all be systematically investigated [15]. Moreover, the nonlinear effects caused by the interaction of magnetic fields and the movement of nanoparticles have to be carefully taken into consideration to guarantee the stable and efficient functioning of the object [16]. Hence, a thorough research that aims at studying thermal performance and magneto-induced flow behavior is necessary in order to close the gap between theoretical and practical engineering applications [17, 18].

The objective of the current study will be to examine the synergistic interaction between magnetic field and nanoparticle dispersion on the fluid flow and heat transfer properties, and this will help to optimize advanced thermal management systems through the proposed study. This paper helps in the formulation of manageable and high-performance heat transfer technology that can be used in the next generation of engineering solutions by analyzing the impact of controlling these physical parameters [19].

The research is presented in a systematic way such that it conducts a thorough research of the magneto nanofluid thermal behavior. The first part gives the basic understanding of nanofluids and magneto hydrodynamic flow and their applicability in the field of engineering. The next part is the mathematical formulation of the problem containing the equations used to model the magneto nanofluid system, the equations governing the problem, and the assumptions employed. This is then succeeded by the methodology part in which the numerical or analytical solution methods are outlined. In this paper, the parameters that affect the velocity and temperature fields the most are analyzed and deemed to be strength of the magnetic field, the concentration of the nanoparticles, and the thermal characteristics. Finally, conclusions are provided, which provide the engineering significance and the potential application of the findings and recommendations on further research.

The following are the Objectives of the Study:
1. To analyze the thermal performance of nanofluids by evaluating enhancements in heat transfer characteristics compared to conventional fluids.
2. To investigate the influence of magnetic fields on nanofluid flow behavior using magneto hydrodynamic principles.
3. To study the combined effects of nanoparticle concentration, Brownian motion, and thermo phoresis on temperature distribution and boundary layer development.
4. To evaluate the impact of key physical parameters such as magnetic parameter, Reynolds number, and thermal conductivity on engineering system efficiency.
5. To provide design insights for practical engineering applications including heat exchangers, cooling systems, and energy devices utilizing magneto nanofluid technology.

II. LITERATURE REVIEW

The studied papers are united together in terms of defining the effect of magnetic fields, nanoparticle composition and flow regimes on heat transfer enhancement, fluid dynamics and energy efficiency. Contrary to the previous traditional-fluid studies, the authors combine experimental, computerized, and AI-aided modeling methods to streamline the thermo-fluid dynamics in complicated physical scenarios. It is also seen in the literature that there is a shift, now towards hybrid systems and ternary nanoparticle systems in order to obtain synergistic thermal properties of the nanofluids. Experimentally, Fe 3 O 4 H2O magnetic nanofluid flow within a copper pipe at a fixed heat flux rate and constant nanoparticle concentration was studied by Erturk et al (2025) [20] and showed that the intensity of magnet field and concentration of nanoparticles were of great importance in enhancing convective heat transfer increasing the Nusselt number by 48.14 percent at Re=7050. Equally, Adogbeji et al. (2025) [21], explored Fe 3 O_2 MgO magnetic hybrid nanofluids under laminar, transition, and turbulent flow conditions and found that they enhanced thermal flux up to 31.6, and that the volume fraction is the factor that causes critical Reynolds numbers to shift. A magnetically-aided ribbed mini-channel heat sink was numerically investigated as a study by Bhattacharyya et al. [22] and improved the heat transfer by almost 65 percent through the synchronized generation and forcing of vortices. Beyond the Newtonian transport, Alraddabi et al. (2025) [23] simulated the magnetized Sisko fluids on a porous stretching cylinder and found that the magnetic fields reduce the velocity with radiation and viscous dissipation increasing the thermal profiles. Rehman et al. (2026) [24] also developed the field by enhancing ternary hybrid nanofluids (THNF) that would exhibit high thermal conductivities and regulated energy dissipations when subjected to squeezing-flow systems applicable in microfluidics and lubrication technology.

The articles examined together are concerned with the problem of the effect of the magnetic fields, the composition of nanoparticles, and the flow regimes on the enhancement of heat transfer and the fluid dynamics and the energy efficiency. In contrast to the previous traditional-fluid studies, Preexisting background and complementary studies (2022 - 2024) were interested in the design of hybrid nanoparticles, thermo physical characterization, and mathematical modeling of magneto-thermal systems. Elfasakhany et al. (2022) [25] studied the rotating $AgMoS_2$ hybrid nanofluids and noted an increase in the temperature transport rate compared to mono-particle nanofluids due to magnetic influence and Kumar et al. (2023) [26] investigated CNT-based magnetized Blasius flow and outlined Joule dissipation as an essential enhancer of thermal transport. Rizwan et al. (2024) [27] studied the use of dielectric oil-based magnetic nanofluids to cool transformers, with a maximum enhancement of dielectric breakdown voltage of 70.05% and associated thermal and electrical as a result. In a study by Irshad et al. (2022) [28], MWCNT + CuO/Therminol55 nanofluids were experimentally prepared and achieves a 128% performance improvement at the cost of viscosity, representing the trade-off between the performance and pumping power. Based on numerical and fractional modeling methods, Hanif et al. (2023) [29] and Muhammad et al. (2023) [30] demonstrated that Nusselt number and thermal efficiency would be highly modified upon the application of Joule heating mechanism, viscous dissipation, and shape factor of nanoparticles, with enhancement to nearly 44.

Sharma and Chaudhary (2025) [31] numerically investigated Cu–H_2O MHD nanofluid flow over an isothermal moving sheet and reported that platelet-shaped nanoparticles exhibited superior heat transfer performance under the combined effects of magnetic field, thermal radiation, and viscous dissipation. More thermo-fluid research highlighted the geometry, convection modes, and interactions of porous media which improve the heat transfer systems. The article by Rasel et al. (2023) [32] simulated mixed convection in a vented chamber; they observed positive increase in Nusselt number (greater than 200 percent) of rotating-cylinder configurations hence underlining the application of geometric control of thermal design. Ismail et al. (2023) [33] demonstrated that the nature of the porosity and radiation parameters is playing a significant role in the hybrid nanofluid flow and skin friction peculiarities of MHD environments. Falkner Skan wedge flow can be examined using viscous dissipation and thermal radiation to confirm a strong correlation of the magnetic parameters with a temperature profile as was done by Adnan et al. (2022) [34]. All these studies demonstrate that significant parameters involved in controlling thermal augmentation are the magnetic field strength, the hybridization of nanoparticles, concentration, and flow configuration. Such issues as pressure decrease, viscosity increase, and higher concentrations stability remain a critical research gap that may be used to encourage future optimization of magneto-nanofluid systems to achieve efficient and sustainable high-performance thermal engineering solutions.

III. RESEARCH METHODOLOGY

The heat transfer of electrically conducting magneto-nanofluids is simulated in a uniform, two-dimensional, laminar and incompressible flow over a uniformly heated flat plate. A uniform transverse magnetic field (B_0) is applied normal to the flow direction to control momentum and heat transfer processes using MHD phenomena. The coupling between the magnetic field and the conducting fluid produces a Lorentz force, which opposes the motion of the fluid and affects the velocity and thermal boundary layer thickness.

The nano fluid is represented as a homogeneous single-phase fluid, assuming uniform nanoparticle distribution and thermal equilibrium between the solid nanoparticles and the base fluid. This model is valid for dilute and well-stabilized nano fluid suspensions, where there is no relative motion between the phases. The presence of the induced magnetic field is neglected because of the small magnetic Reynolds number, and the dominant electromagnetic interaction is controlled by the externally applied magnetic field. Figure 2 presents the Framework of proposed methodology.

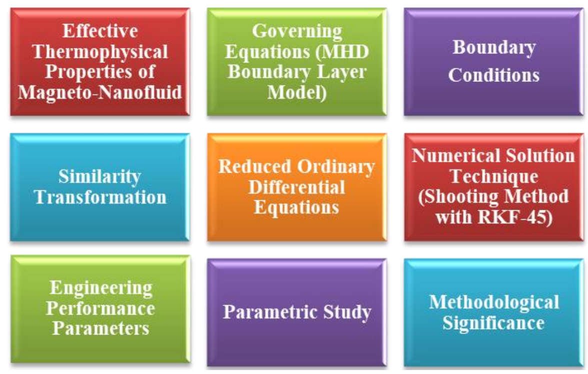

Fig 2: Framework of Proposed Methodology

3.1. Effective Thermophysical Properties of Magneto-Nanofluid

A classic mixture model (treats as homogeneous, single-phase) is used to evaluate effective thermo physical properties of the magneto-nanofluid using a single mixture model where the mixture is treated as homogeneous. The classic mixture model is acceptable for dilute nanofluids where nanoparticles are uniformly distributed and at thermal equilibrium with the base fluid.

The effective density of a nanofluid is determined through volumetric averaging of the fluid phase and solid phase and can be expressed mathematically as follows:

$$p_{nf} = (1 - \emptyset)p_f + \emptyset p_s \qquad (1)$$

where $\emptyset$ represents the volume fraction of nanoparticle, while p_f and p_s represent the densities of the base fluid and solid nanoparticles, respectively.

The dynamic viscosity (μ_n) is calculated using the Brinkman equation accounting for increased flow resistance due to the presence of particles in suspension; thus, it can be concluded that viscosity increases in a non-linear manner with increase in number of particles:

$$\mu_{nf} = \frac{\mu_f}{(1-\emptyset)^{2.5}} \qquad (2)$$

The effective heat capacity of the nanofluid, or energy that can be stored in this material mixture, and can be calculated mathematically as follows:

$$(\rho C_p)_{nf} = (1 - \emptyset)(\rho C_p)_f + \emptyset(\rho C_p)_s \qquad (3)$$

To illustrate enhancement to thermal transport, the Maxwell model is utilized to describe effective thermal conductivity:

$$\mathrm{k_{nf}} = \mathrm{k_f}\left[\frac{\mathrm{k_s}+2\mathrm{k_f}-2\emptyset(\mathrm{k_f}-\mathrm{k_s})}{\mathrm{k_s}+2\mathrm{k_f}+\emptyset(\mathrm{k_f}-\mathrm{k_s})}\right] \qquad (4)$$

The above-mentioned equations will provide a quantitative understanding of how density, dynamic viscosity, effective heat capacity, and effective thermal conductivity are all influenced by the introduction of magnetic nanoparticles; thus, enhancing momentum diffusion and heat diffusion properties as required for thermally regulated magnetic systems.

3.2. Governing Equations (MHD Boundary Layer Model)

The flow and heat transfer characteristics of the magneto-nanofluid are defined by the boundary-layer approximation of the MHD conservation equations [35]. For steady two-dimensional incompressible flow, continuity ensures mass conservation within the boundary layer and is expressed as:

$$\frac{\partial u}{\partial x} + \frac{\partial v}{\partial y} = 0 \qquad (5)$$

The momentum equation includes viscous diffusion and thermal electromagnetic interaction effects. Under a transverse magnetic field, it reduces to:

$$u\frac{\partial u}{\partial x} + v\frac{\partial u}{\partial y} = V_{nf}\ \frac{\partial^2 u}{\partial y^2} - \frac{\sigma_{nf} B^2{}_0}{\rho_{nf}}\ u \qquad (6)$$

The last term represents the Lorentz force,

$$F_L = \sigma_{nf} B^2{}_0 u \qquad (7)$$

which acts against fluid motion, hence increasing the thickness of the momentum boundary layer and providing a means for magnetic control of transport behavior.

The thermal field is described by an energy equation that includes convective and conductive heat transfer in the nanofluid:

$$u\frac{\partial T}{\partial x} + v\frac{\partial T}{\partial y} = \propto_{nf}\ \frac{\partial^2 T}{\partial y^2} \qquad (8)$$

V_{nf} is taken as the effective kinematic viscosity and $\propto_{nf}$ is the thermal diffusivity of nanofluid defined in turn as:

$$V_{nf} = \frac{\mu_{nf}}{\rho_{nf}}, \quad \propto_{nf} = \frac{k_{nf}}{(\rho C_p)_{nf}} \qquad (9)$$

These coupled equations represent hydrodynamic, thermal, and electromagnetic mechanism interactions which form a basic mathematical model for studying magnetically influenced nanofluid flow and heat transfer over a heated surface [36].

3.3. Boundary Conditions

The boundary conditions are defined to represent the physical interaction between the magneto-nanofluid and the heated surface. At the wall (y = 0), a no-slip condition is imposed, which assumes that the fluid adheres to the surface; therefore, the velocity components satisfy u = 0 and v = 0. The surface is maintained at a constant temperature T = T_w, modeling an isothermal heating condition commonly used in engineering thermal systems.

Far away from the surface (y → ∞), the influence of the wall diminishes, and the fluid approaches the free-stream conditions. Accordingly, the velocity tends toward the ambient flow velocity $u \rightarrow U_\infty$, while the temperature approaches the surrounding fluid temperature $T \rightarrow T_\infty$. These boundary conditions ensure a realistic description of boundary-layer development and enable the evaluation of surface shear stress and convective heat transfer characteristics.

3.4. Similarity Transformation

Similarity transformations are also used to reduce the complexity of the mathematical analysis to a system of ordinary differential equations by transforming the governing partial differential equations. Similarity variable is proposed as:

$$\eta = y\sqrt{\frac{U_\infty}{V_{nf} x}} \qquad (10)$$

that integrates the spatial coordinates into a lone dimensionless parameter and allows the self-similar solutions of the boundary-layers. A stream function ψ is a function defined by the following property:

$$\psi = \sqrt{U_\infty V_{nf} x\, f(\eta)} \qquad (11)$$

solving automatically the continuity equation. With this transformation, the velocity components could be expressed as:

$$u = U_\infty f'(\eta),\ v = \frac{1}{2}\sqrt{\frac{V_{nf} x\, U_\infty}{x}}\,[n^{f'}(\eta) - f(\eta)] \qquad (12)$$

The temperature field is non-dimensionalized through

$$\theta(\eta) = \frac{T - T_\infty}{T_w - T_\infty} \qquad (13)$$

The normalized thermal profile in the boundary layer which is denoted by these simplifications make the model less complicated and the fundamental physics of magneto-nanofluid flow and heat transfer remains intact.

3.5. Reduced Ordinary Differential Equations

Upon the transformations of similarity, the governing equations of the boundary-layer equations are simplified to a group of coupled nonlinear ordinary differential equations [37]. The changed momentum equation takes the following form:

$$f''' + \frac{1}{2} ff'' - Mf' = 0 \qquad (14)$$

while the energy equation becomes:

$$\theta'' + \Pr f\theta' = 0 \qquad (15)$$

Here, M is the Hartmann number, defined as:

$$M = \frac{\sigma_{nf} B^2{}_0}{\rho_{nf} U_\infty} \qquad (16)$$

the ratio of the applied magnetic field to viscous forces and the magnetic damping of the flow, and is equal to the ratio of the magnetic field H to the viscous force ver times the ratio of the magnetic field H to the force of viscosity times the square of the ratio of the magnetic field H to the force of viscosity.

The Prandti number is expressed as the value of Pr.

$$\Pr = \frac{V_{nf}}{\propto_{nf}} \qquad (17)$$

indicating the ratio of momentum diffusivity to thermal diffusivity. These dimensionless parameters control the influence of electromagnetic effects and thermal transport within the magneto-nanofluid boundary layer.

3.6. Numerical Solution Technique (Shooting Method with RKF-45)

The transformed boundary-value problem is solved numerically by converting it into an equivalent initial-value problem using the shooting method. The unknown initial slopes $f''(0) = s_1$ and $f''(0) = s_1$ are first guessed and then iteratively adjusted so that the far-field boundary conditions $f'(\infty) = 1$ and $\theta(\infty) = 0$ are satisfied. The resulting system of first-order differential equations is integrated using the Runge–Kutta–Fehlberg (RKF-45) [38] scheme, which provides high accuracy and numerical stability through adaptive stepwise evaluation:

$$y_{n+1} = y_n + \frac{h}{6}(k_1 + 2k_2 + 2k_3 + k_4) \qquad (18)$$

The intermediate slope estimates Known as $k_1,\ k_2,\ k_3$ and k_4 are calculated for each iteration and the iterations are repeated until the final error (residual) is less than $|Residual| < 10^{-6}$ via convergence. Thus, allowing for accurate calculations of velocity and temperature profiles in the boundary layer of the magneto-nanofluid.

3.7. Engineering Performance Parameters

The performance of the magneto-nanofluid flow in engineering is assessed through dimensionless quantities that represent surface drag and heat transfer efficiency [39]. The skin friction coefficient is given by:

$$C_f = \frac{T_w}{\rho U^2{}_\infty} \qquad (19)$$

where the wall shear stress is given by:

$$T_w = \mu_{nf}\left(\frac{\partial u}{\partial y}\right)_{y=0} \qquad (20)$$

In similarity form, the skin friction coefficient relates directly to the second derivative of the dimensionless stream function at the wall, $C_f = \propto f''(0)$ thus indicating how much influence magnetic field and nanoparticle concentration have on surface resistance.

Heat transfer is quantified by using local Nusselt number,

$$N_{u_x} = \frac{x\, q_w}{k_{nf}\,(T_w - T_\infty)} \qquad (21)$$

where the surface heat flux is:

$$q_w = -k_{nf}\left(\frac{\partial T}{\partial y}\right)_{y=0} \qquad (22)$$

In similarity variables, this reduces to $N_{u_x} \propto -\theta'(0)$, which thermal gradient at the wall governs convective heat transfer enhancement.

These are key parameters that describe a trade-off between improvements in heat transfer and resistance to flow for magnetically controlled nanofluid systems.

3.8. Parametric Study

The parametric analysis is conducted fully to determine the effect of the key dimensionless parameters i.e., volume fraction of nanoparticles $\emptyset$ magnetic parameter M and Prandtl number Pr. These are methodically adjusted to determine their impact on flow and thermal characteristics especially velocity suppression due to magnetic damping, a change in thickness of the boundary-layer, a rise in convective heat transfer, as well as a modification in the surface drag characteristics. With this study, the most effective operating conditions can be established in order to obtain a thermal performance and simultaneously a reasonable hydrodynamic resistance in magneto-nanofluids-based systems in the field of engineering.

The specified approach assumes the use of the nanofluids transport theory MHD flow control, similarity analysis, and the high-order numerical calculation to create an overall predictive scheme in the analysis of magnetically controlled systems of heat transfer. The model also provides useful design insights to the advanced engineering programs, the microchannel cooling, energy conversion device, aerospace thermal protection, and smart heat exchangers that must be thermally controlled with great care by term of thermal enhancement mechanisms and the magnetic field modulation. The given methodology incorporates the nanofluid transport theory, magnetohydrodynamic (MHD) flow control, similarity analysis, and the high-order numerical calculation to derive the overall predictive scheme to the process of magnetically controlled heat transfer. The model provides useful design data to the advanced engineering applications, such as the microchannel cooling, energy conversion devices, aerospace thermal protection systems and smart heat exchangers which must be carefully thermally regulated by thermal enhancement mechanisms and magnetic field modulation.

IV. RESULTS

Figure 3 shows an increasing trend in the relationship between Cf (coefficient of friction) and M. The value of M increases between 0-3 as Cf r increases between 0.42 and 0.55. At Cf = 0.42, M = 0, which means that there is no observed effect. As Cf becomes 0.46, M r grows to 1, indicating an early growth. Moreover, M = 2 at Cf = 0.50 which shows a proportional and consistent increase. When Cf = 0.55, which is the largest value, the value of M = 3, the maximum.

The difference between data points is constant, which means that it is linear. In general, the graph indicates a positive association between the coefficient of friction and M in that, at high Cf values, the graph indicates that the values of M are high.

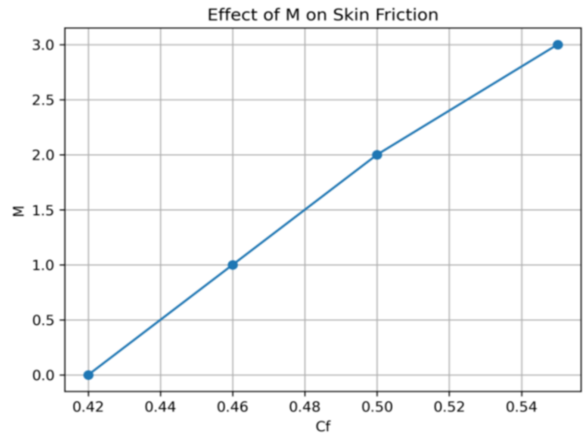

Figure 3: Linear relationship between Cf and M

Figure 4 shows the change in velocity and temperature profiles with respect to similarity variable eta. In η = 0, the velocity begins with 0 and grows very fast, with a maximum of about 0.6 at η = 1 and 0.9 at η= 2. It tends towards unity (=1.0) as eta further increases beyond 4, which suggests a constant state. Conversely, the temperature profile starts with a value of 1.0 when η = 0 and drops to almost zero at eta = 0.005 and 0.2 at 0.001. It also tends toward zero as η tends towards 6-10. This shows that there is an inverse relationship between the velocity and temperature profiles against η.

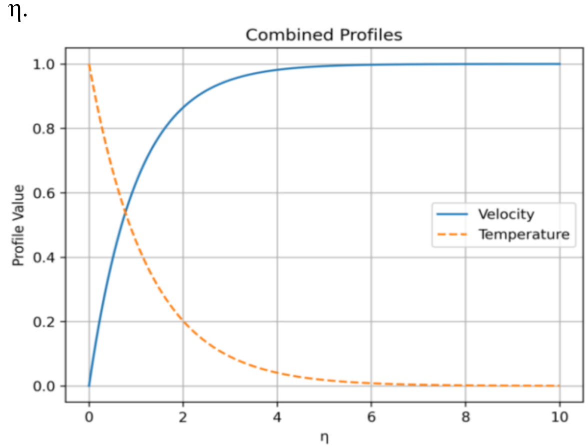

Figure 4: Velocity and temperature profiles variation with similarity variable η

Figure 5 illustrates the comparison of two engineering parameters Cf and Nu based on a bar chart. Cf (skin friction coefficient) is about 0.47 which shows that the friction level is moderate at the surface. Nevertheless, Nu (Nusselt number) is slightly bigger (approximately 0.52) which corresponds to a more intense heat transfer rate. The two parameters differ by approximately 0.05 implying that Nu is slightly higher than Cf. The two values are closely close ranging between 0.45 and 0.55 implying that it possesses balanced fluid movement and heat transfer properties. On the whole, the chart shows that the performance of heat transfer (Nu) is slightly greater compared to that of the frictional effect (Cf).

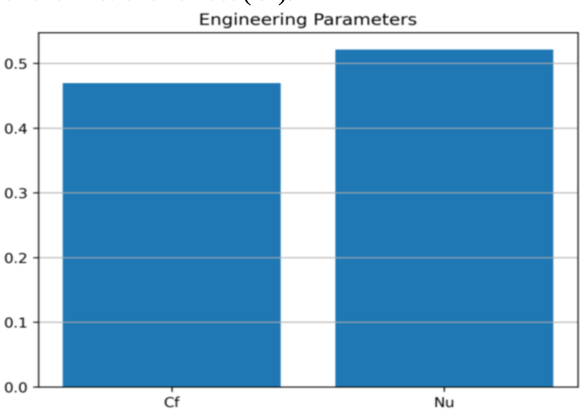

Figure 5: Comparison of engineering parameters Cf and Nu

Figure 6 shows the effect of the Prandtl number (Pr) on heat transfer represented by the Nusselt number (Nu). The higher Nu goes, the higher the Pr becomes, that is, as Nu goes up, with Nu reaching 0.30, Pr increases dramatically, say to 6.2, then to 18.50, and so on. Nu = 0.30 gives a low thermal diffusivity ratio of Pr = -0.7. As Nu increases to 0.40, Pr increases gradually to 1.0. Higher increment can be seen at Nu = 0.48, where Pr takes a value of 3.0. Lastly, Pr reaches its highest at Nu = 0.52 at an approximate of 6.2, which suggests a significant improvement. The trend shows nonlinear and accelerating dependency with higher Nu values indicating accelerated increase in Pr which indicates enhanced heat transfer features.

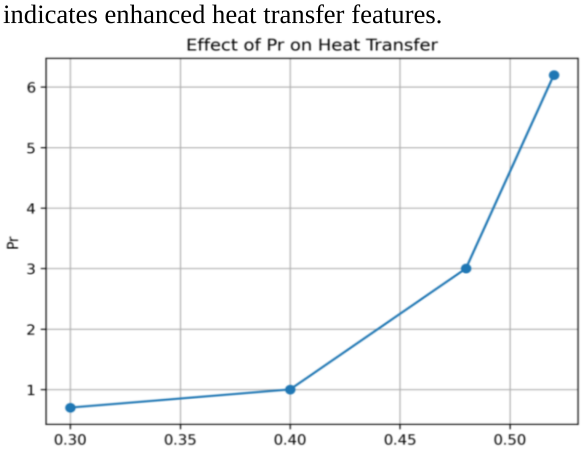

Figure 6: Effect of Prandtl number on heat transfer (Nu)

Figure 7 represents the plot of 0eta -1 theorem as a proportional function of eta between 0 and 10. At η = 0, θ′(η) starts near −0.78. With increasing η, the θ(η) continuously increases towards zero, which means that the negative gradient decreases. Around η ≈ 1, the value is about −0.4, and by η ≈ 2 it is near −0.2. The curve keeps rising in a slower and slower manner to a point of about -0.05 at eta = 4. Beyond η ≈ 5, the values approach zero asymptotically, with θ′(η) ≈ −0.01 to 0 by η = 8–10.

The magnitude of the slope reduces progressively, with a rapid change at small η, but with a very slow change at large eta. In general, the curve is a decay of magnitude toward zero of an exponential type.

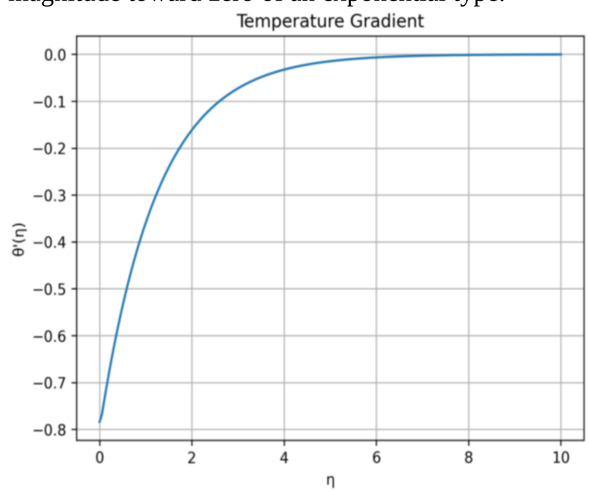

Figure 7: Temperature gradient profile θ′(η) as a function of η from 0 to 10.

Figure 8 illustrates that 0 0 0 eta eta eta (eta) reduces as eta increases in the range of 0 0 0 eta eta (eta) 0 eta eta (eta). At η = 0, θ(η) begins at 1.0. This means that as η goes up, 0.e.t (eta) decreases exponentially and takes the values of about 0.6 when eta is around 1 and 0.2 when eta is around 2.

The rate of decrease slows beyond η ≈ 2, with θ(η) ≈ 0.08 at η ≈ 3 and around 0.03–0.04 at η ≈ 4. In the 5-6 region, η (5-6) is less than 0.02, and it is heading towards zero at an asymptotic. By η ≈ 8–10, θ(η) is nearly zero.

The curve is an exponential-shaped decay, monotonic and smooth, with the sharpest gradient at the point η = 0, and the changes are becoming smaller with the increase of η.

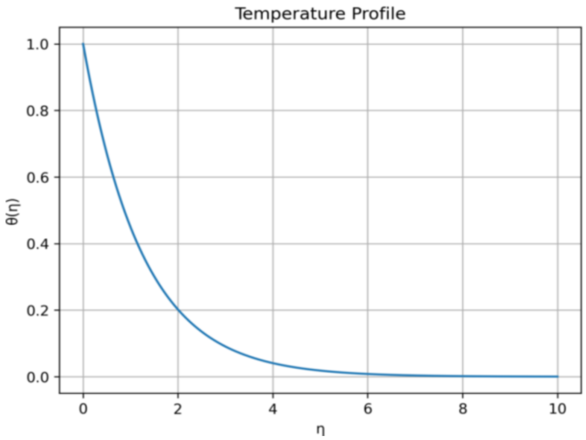

Figure 8: Variation of temperature profile θ(η) showing exponential decay toward zero with increasing η.

The Figure 9 shows θ(η) for four Prandtl numbers: Pr = 0.7, 1, 3, and 6.2. Each of the curves begins at 0 = 1 and moves monotonically to zero with increase in eta. For Pr = 0.7, θ(η) ≈ 0.6 at η ≈ 1, 0.45 at η ≈ 2, and 0.2 at η ≈ 4. For Pr = 1, values drop faster, reaching about 0.5 at η ≈ 1 and 0.1 at η ≈ 4. For Pr = 3, θ(η) ≈ 0.4 at η ≈ 1 and falls below 0.05 by η ≈ 4. The steepest decay occurs for Pr = 6.2, where θ(η) ≈ 0.3 at η ≈ 1 and nearly zero by η ≈ 4. Increased Pr leads to a reduction in thickness of thermal layers and temperature decay.

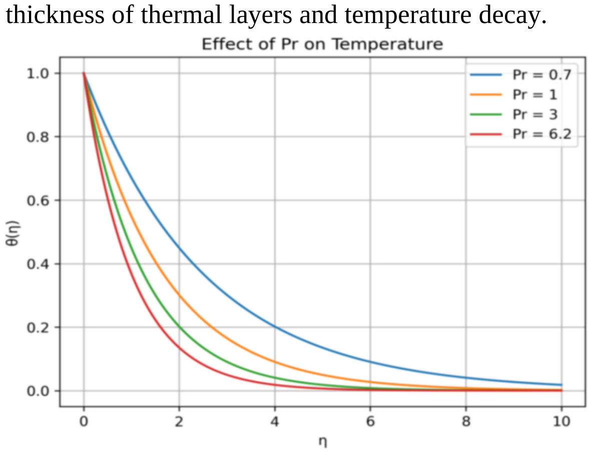

Figure 9: Influence of Prandtl number on temperature profile, showing faster decay with increasing Pr.

Figure 10 illustrates the change in f 3(eta)/ eta at 0 of eta to 10 of eta. f 2 (0) begins close to 0.98, corresponding to a large starting shear stress on the surface. As eta rises, the value declines very quickly and reaches about 0.5 when eta is just about 1 and about 0.15 when eta is just about 2. The decay continues with f″(η) ≈ 0.05 at η ≈ 3 and around 0.02 at η ≈ 4. Outside of η 5, the values tend towards zero, but the variation between eta between 6 and 10 is insignificant. The curve exhibits a smooth, exponential-like decay of a monotonic nature and the gradient of the curve becomes steepest at η = 0 and then gradually becomes less steep as η increases.

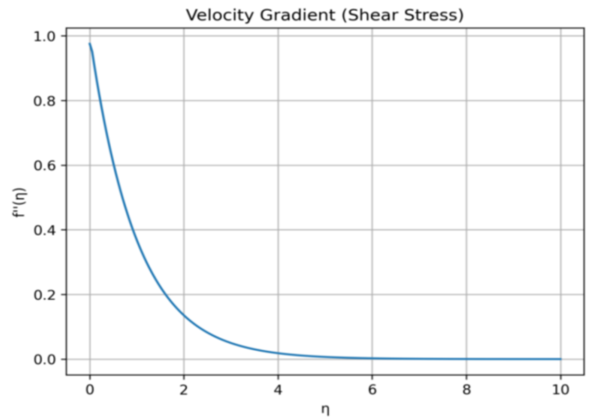

Figure 10: Variation of velocity gradient f″(η) indicating rapid decay of shear stress away from the surface.

Figure 11 shows how the velocity profile f 7 (η) changes with η in the range 0 = 0 and 10 = 10. The value of f'''(η) at 0 is 0 which is the surface no-slip. With increasing η, the velocity increases at a high rate, culminating at some 0.6 in η 1, and 0.85 in η 2. The growth rate then slows, with f′(η) ≈ 0.95 at η ≈ 3 and around 0.98 at η ≈ 4. Increasingly beyond η = 5, the curve tends to the asymptotic value of unity, with f(η) 8 between η = 6 and 10, f(eta) = 0.99 -1.0. The profile is monotonic smooth with a sharp rise near the wall and then stabilization gradually leading to the development of the boundary layer up to the free-stream velocity.

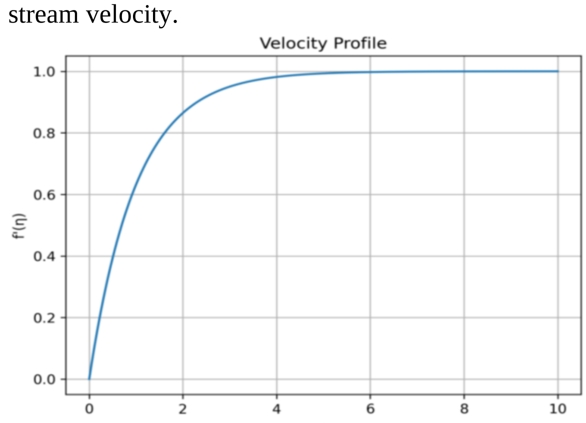

Figure 11: Velocity profile f′(η) increasing to unity with η.

Figure 12 presents velocity profiles (f'(η)) for magnetic parameter values (M = 0, 1, 2,) and (3). All curves start at (f'(0) = 0), which is the no-slip condition and moves monotonically towards unity as (eta) rises. For (M = 0), the velocity increases rapidly, reaching about 0.7 at (η \approx 1) and 0.95 at (η \approx 3). The greater is the magnetic parameter, the slower is the velocity growth. For (M = 1), (f'(η) \approx 0.6) at (η \approx 1) and 0.9 at (η \approx 3), while for (M = 2), the values decrease further. The least acceleration is of (M = 3) the velocity approaching unity more slowly. This action suggests that the flow is impeded by the magnetic action increased (M) and the momentum boundary layer becomes thicker.

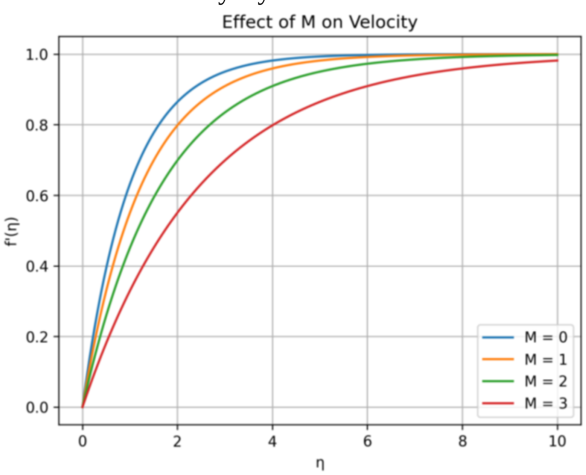

Figure 12: Effect of magnetic parameter M showing reduced velocity growth with increasing M.

V. CONCLUSION

The present study is a thorough inquiry into the magneto-nanofluid flow, and thermal behavior when an external magnetic field is applied to it. The findings reveal a clear indication that the introduction of nanoparticles tremendously increases the thermal conductivity and the rate of heat transfer when compared to the traditional fluids and are therefore highly recommended in the contemporary high-efficiency thermal systems. When a magnetic field is applied, Lorentz forces are induced and these forces are effective in controlling fluid motion, causing velocity to be reduced and momentum boundary layer to increase. Moreover, Prandtl numbers were observed to increase the performance of heat transfer by reducing the thermal boundary layer and increased nanoparticle concentration increased heat transport at the cost of increased viscosity and pumping power. Similarity transformations, RKF-45 shooting technique, the numerical methodology was accurate and reliable in solving the nonlinear governing equations. Engineering wise, the study has beneficial design information on how to optimize engineering systems like heat exchangers, microchannel cooling device and renewable energy.

But this is faced with challenges of nanoparticle stability, agglomeration and pressure drop increase. Experimental validation and hybrid nanofluid development with multi-physics optimization should be the future work whether to make sure that the system can be implemented practically and make the thermal system design sustainable.

REFERENCES

[1] Abdullaev, R. N., A. Sh. Agazhanov, A. R. Khairulin, D. A. Samoshkin, and S. V. Stankus, "Thermophysical properties of magnesium in solid and liquid states," *J. Eng. Thermophys.*, vol. 31, no. 3, pp. 384–401, 2022.

[2] M. Akram, W. Jamshed, B. S. Goud, A. A. Pasha, T. Sajid, M. M. Rahman, M. Arshad, and W. Weera, "Irregular heat source impact on Carreau nanofluid flowing via exponential expanding cylinder: A thermal case study," Case Stud. Therm. Eng., vol. 36, Art. no. 102171, 2022.

[3] J. Yang, X. Yang, J. Wang, H. H. Chin, and B. Sundén, "Review on thermal performance of nanofluids with and without magnetic fields in heat exchange devices," Front. Energy Res., vol. 10, Art. no. 822776, 2022.

[4] W. Jamshed et al., "The improved thermal efficiency of Prandtl–Eyring hybrid nanofluid via classical Keller box technique," Sci. Rep., vol. 11, no. 1, Art. no. 23535, 2021.

[5] G.-Y. Jeong, S. P. Jang, H.-Y. Lee, J.-C. Lee, S. Choi, and S.-H. Lee, "Magnetic-thermal-fluidic analysis for cooling performance of magnetic nanofluids comparing with transformer oil and air by using fully coupled finite element method," IEEE Trans. Magn., vol. 49, no. 5, pp. 1865–1868, 2013.

[6] H. Khelifa, A. Beroual, and E. Vagnon, "Effect of conducting, semi-conducting and insulating nanoparticles on AC breakdown voltage and partial discharge activity of synthetic ester: A

statistical analysis," Nanomaterials, vol. 12, no. 12, Art. no. 2105, 2022.

[7] D.-E. A. Mansour, A. M. Elsaeed, and M. A. Izzularab, "The role of interfacial zone in dielectric properties of transformer oil-based nanofluids," IEEE Trans. Dielectr. Electr. Insul., vol. 23, no. 6, pp. 3364–3372, 2016.

[8] M. H. A. Hamid, M. T. Ishak, M. F. Md Din, N. S. Suhaimi, and N. I. A. Katim, "Dielectric properties of natural ester oils used for transformer application under temperature variation," in Proc. IEEE Int. Conf. Power Energy (PECon), 2016, pp. 54–57.

[9] M. Ouni, L. M. Ladhar, M. Omri, W. Jamshed, and M. R. Eid, "Solar water-pump thermal analysis utilizing copper–gold/engine oil hybrid nanofluid flowing in parabolic trough solar collector: Thermal case study," Case Stud. Therm. Eng., vol. 30, Art. no. 101756, 2022.

[10] Z. B. Siddique and P. Basak, "Transformer design considerations for green renewable dielectric nanofluid," IEEE Trans. Dielectr. Electr. Insul., vol. 31, no. 2, pp. 1110–1113, 2024.

[11] N. S. Suhaimi et al., "A review on palm oil-based nanofluids as a future resource for green transformer insulation system," IEEE Access, vol. 10, pp. 103563–103586, 2022.

[12] A. Thabet, S. A. Shaaban, and M. Allam, "Enhancing dielectric constant of transformer oils using multi-nanoparticles technique under thermal conditions," in Proc. 18th Int. Middle East Power Syst. Conf. (MEPCON), 2016, pp. 220–225.

[13] N. A. Shah et al., "Effect of generalized thermal transport on MHD free convection flows of nanofluids: A generalized Atangana-Baleanu derivative model," Case Stud. Therm. Eng., vol. 40, Art. no. 102480, 2022.

[14] F. Shahzad et al., "Thermal analysis characterisation of solar-powered ship using Oldroyd hybrid nanofluids in parabolic trough solar collector: An optimal thermal application," Nanotechnol. Rev., vol. 11, no. 1, pp. 2015–2037, 2022.

[15] H. Yang et al., "Thermal inspection for viscous dissipation slip flow of hybrid nanofluid (TiO_2–Al_2O_3/$C_2H_6O_2$) using cylinder, platelet and blade shape features," Sci. Rep., vol. 13, no. 1, Art. no. 8316, 2023.

[16] M. Zaydan, A. Wakif, A. Alshehri, T. Muhammad, and R. Sehaqui, "A passive modeling strategy of steady MHD reacting flows for convectively heated shear-thinning/shear-thickening nanofluids over a horizontal elongating flat surface via Wakif's-Buongiorno approach," Numer. Heat Transfer A Appl., pp. 1–24, 2024.

[17] M. Rajnak et al., "Transformer oil-based magnetic nanofluid with high dielectric losses tested for cooling of a model transformer," IEEE Trans. Dielectr. Electr. Insul., vol. 26, no. 4, pp. 1343–1349, 2019.

[18] T. O. Scott, D. R. E. Ewim, and A. C. Eloka-Eboka, "Hybrid nanofluids flow and heat transfer in cavities: A technological review," Int. J. Low-Carbon Technol., vol. 17, pp. 1104–1123, 2022.

[19] H. Ertürk and T. Koca, "Investigation of thermal performance of Fe_3O_4 nanofluid applied with magnetic field under constant heat flux," J. Therm. Anal. Calorim., pp. 1–13, 2025.

[20] V. O. Adogbeji, M. Sharifpur, and J. P. Meyer, "Experimental investigation of heat transfer, thermal efficiency, pressure drop, and flow characteristics of Fe_3O_4-MgO magnetic hybrid nanofluid in transitional flow regimes," Int. J. Therm. Sci., vol. 209, Art. no. 109515, 2025.

[21] S. Bhattacharyya et al., "Magneto-hydrodynamic behavior of magnetic nanofluids in mini-channel heat sinks for electronics cooling," Sci. Rep., vol. 15, no. 1, Art. no. 28861, 2025.

[22] I. Alraddadi, S. M. Hussain, and M. Khan, "Thermal transport and fluid flow analysis of Magneto-Sisko fluid through porous medium under radiation effects using ANN-based and numerical approaches," Case Stud. Therm. Eng., Art. no. 107584, 2025.

[23] A. Rehman et al., "Semi-numerical simulation for the thermal performance of unsteady squeezing non-Newtonian MHD couple stress ternary hybrid nanofluid flow between parallel surfaces," Int. J. Thermofluids, vol. 31, Art. no. 101516, 2026.

[24] A. Elfasakhany et al., "Thermal energy investigation of magneto-hydrodynamic nano-material liquid flow over a stretching sheet: Comparison of single and composite particles," Alex. Eng. J., vol. 61, pp. 10453–10462, 2022.

[25] T. K. Kumar and M. D. Shamshuddin, "Thermal performance on radiative and ohmic dissipative magneto-nanoliquid over moving flat porous plate suspended by single wall carbon nanotubes and multi wall carbon nanotubes," J. Nanofluids, vol. 12, no. 1, pp. 192–201, 2023.

[26] M. Rizwan, S. A. Khan, M. R. Khan, and A. A. Khan, "Experimental and statistical investigation on the dielectric breakdown of magneto nanofluids for power applications," J. Mater. Sci.: Mater. Eng., vol. 19, no. 1, p. 5, 2024.

[27] K. Irshad et al., "Thermal performance investigation of Therminol55/MWCNT+CuO nanofluid flow in a heat exchanger from an exergy and entropy approach," Case Stud. Therm. Eng., vol. 34, Art. no. 102010, 2022.

[28] H. Hanif et al., "Numerical Crank-Nicolson methodology analysis for hybridity aluminium alloy nanofluid flowing based-water via stretchable horizontal plate with thermal resistive effect," Case Stud. Therm. Eng., vol. 42, Art. no. 102707, 2023.

[29] S. Muhammad, T. Anwar, Asifa, and M. Yavuz, "Comprehensive investigation of thermal and flow features of alloy based nanofluid considering shape and Newtonian heating effects via new fractional approach," Fractal Fract., vol. 7, no. 2, Art. no. 150, 2023.

[30] S. Sharma and S. Chaudhary, "Computational analysis of MHD copper-water nanofluid with effect of viscous dissipation and thermal radiation over isothermal moving sheet," Indian J. Pure Appl. Phys., vol. 63, no. 7, pp. 638–647, 2025.

[31] M. S. Rasel, M. T. I. Rupam, M. S. Shuvo, and S. Saha, "Investigation on conjugate mixed convection through a vented chamber with heat generating and conducting rotating circular cylinders," Results Eng., vol. 19, Art. no. 101248, 2023.

[32] M. Ismail and D. M. Gururaj, "Numerical investigation on nonlinear radiative magneto hydrodynamics hybrid nanofluid flow past a stretching cylinder embedded in porous medium," J. Nanofluids, vol. 12, no. 3, pp. 809–818, 2023.

[33] M. Adnan, R. Hussain, Z. Rehman, I. Khan, and M. Andualem, "Thermal enhancement in Falkner–Skan flow of the nanofluid by considering molecular diameter and freezing temperature," Sci. Rep., vol. 12, no. 1, Art. no. 9415, 2022.

[34] K. Bhattacharyya and I. Pop, "MHD boundary layer flow due to an exponentially shrinking sheet," Magnetohydrodynamics, vol. 47, no. 4, pp. 337–344, 2011.

[35] M. S. Khan, I. Karim, M. S. Islam, and M. Wahiduzzaman, "MHD boundary layer radiative, heat generating and chemical reacting flow past a wedge moving in a nanofluid," Nano Converg., vol. 1, no. 1, Art. no. 20, 2014.

[36] S.-B. Hsu and K.-C. Chen, Ordinary Differential Equations with Applications, vol. 23. Singapore: World Scientific, 2022.

[37] K. M. Nihaal, U. S. Mahabaleshwar, N. Swaminathan, D. Laroze, and I. V. Shevchuk, "A numerical investigation of activation energy impact on MHD water-based Fe_3O_4 and $CoFe_2O_4$ flow between the rotating cone and expanding disc," Mathematics, vol. 12, no. 16, Art. no. 2530, 2024.

[38] D. L. Pillay et al., "Engineering performance of metakaolin based concrete," *Cleaner Eng. Technol.*, vol. 6, Art. no. 100383, 2022.